



New route for synthesis of pure anatase TiO₂ nanoparticles via ultrasound-assisted sol-gel method

Saja S. Al-Taweel* and Haider R. Saud

Chemistry Department, College of Science, AL- Qadisiyah University, Dewanyia, Iraq

ABSTRACT

Anatase phase of Titanium dioxide nanoparticles (TiO₂-nps) was prepared by new route using ultrasound assisted sol-gel method with operating conditions (40 kHz, 350 W). The crystal phase, morphology, surface area, thermal properties, and optical properties of TiO₂-nps were characterized by X-ray diffraction (XRD), FTIR spectroscopy, Raman spectroscopy, scanning electron microscopy (SEM), transmission electron microscopy (TEM), atomic force microscopy (AFM), BET & BJH surface analysis, thermogravimetric analysis (TGA), and UV-Vis absorption spectroscopy. The synthesized nanoparticles have mesopores-micropores surface with pure anatase phase and small crystal size (approximately 11nm). The spherical shape of TiO₂-nps can be examined through the SEM, TEM, and AFM images. The synthesized TiO₂-nps have highly thermal stability (mass loss ≈ 0 until 542°C), the surface area and band gap values of TiO₂-nps were calculated to be 64.041 m²/g and 3.2 eV respectively.

Keywords: TiO₂, anatase, nanoparticles, ultrasound synthesis

INTRODUCTION

Titanium dioxide is one of the most important semiconductors have a wide range of applications like, superhydrophilic coatings, solar cell and sonocatalysis or photocatalysis for water purification [1-3]. Among different types of photocatalysts, TiO₂ has unique properties such as, photoactivity, resistant to chemical corrosion, resistant to poisoning, and deactivation [4-6]. TiO₂ with nanostructures show a remarkable physiochemical properties, significantly different from bulky structure, like large specific surface area, extremely small size of particles, and quantum size effect [7]. Recently, there's a considerable interest in the synthesis of titanium dioxide nanoparticles with pure anatase phase [8]. As reported, the anatase phase is the more favorable structure than the two polymorphs (rutile, and brookite) due to its high photoactivity [9,10].

Various methods have been used to synthesis nanosized TiO₂, such as sol-gel, hydrothermal, solvothermal, and sonochemical [11-14]. The sol-gel method is the most famous and flexible route for the production of nano metal oxide via inorganic precursor (i.e. TiCl₄) or organometallic precursor (i.e. Ti(O-alkyl)₄) [15,16]. Additionally, the particle size and shape of nanoparticles can be extensively varied in a controlled manner by selecting different sol-gel process parameters, including pH nature, and molar ratio of water/alkoxide, type of additives, and the solvent nature [17,18]. In spite of a simplicity of sol-gel technique, some drawback limit its performance in nanoparticles synthesis such as spontaneous aggregation of primary particles, and small surface area of synthesized TiO₂ nanoparticles [19]. In addition, one of the characteristic property of titanium dioxide its ability to aggregate into large particle size via chemical bounds [20]. Ultrasound is the most effective method for preventing aggregation and powerful tool for dispersing of particles in heterogeneous systems [21]. The extreme conditions during sonication

process lead to highly mixing, the particles size of solid present in sonochemical reactor decrease and the reactive surface area becomes greeter [22]. There is two ultrasonic Effects on synthesis of nanomaterials includes; the ultrasonic effect on nucleation and growth of solid particles that generated from liquid phase [23], and the effect of ultrasonic on synthesis involving dissolution-reprecipitation process [24].

In this work we investigate a new route to synthesize pure anatase TiO₂ nanoparticles from suitable precursor titanium tetraisopropoxide. The synthesis was performed under ultrasound irradiation at low temperature. The choice of ultrasound assisted sol-gel as a method for synthesis of TiO₂ nanoparticles is motivated by both size reduction of particles and production purely anatase TiO₂ phase.

EXPERIMENTAL SECTION

Materials

Isopropyl alcohol ((CH₃)₂CHOH, 99.5%), hydrochloric acid (HCl, 37%), were purchased from BDH. Titanium (IV) isopropoxide (Ti[OCH(CH₃)₂]₄, 97%) was purchased from Sigma-Aldrich. All chemicals were used without further purification.

Synthesis of anatase TiO₂ nanoparticles

10 mL of the Titanium isopropoxide (TTIP) as a precursor was mixed with 40 mL isopropyl alcohol and stirred for 30 min. Then 10 mL of a mixture (1:1) of deionized water and isopropyl alcohol was added drop wisely into the TTIP mixture to form colloidal solution under vigorous stirrer. The pH of the obtained colloidal solution was adjusted to 3 and irradiated by ultrasound using Ultrasonic water bath (Hwasin Technology Powersonic 405, Korea, 40 kHz, 350 W) for 30 min. the colloidal solution was dried in an oven at 110°C for 3 h, and the obtained xerogel was calcinated at 450°C for 3h.

Characterization of TiO₂ nanoparticles

The crystalline phase of titania nanoparticles (TiO₂-nps) was characterized by XRD using (Bruker AXS GmbH, Germany/D2 Phaser) with CuK_α radiation (0.15040nm), the XRD pattern was recorded from 20 to 70°. Raman spectra of TiO₂-nps was performed using Bruker micro-Raman (senterra, Germany) with wavelength of irradiation 785nm. To determine the functional groups of TiO₂, FTIR (Shimadzu FTIR 8400s, Japan) analysis was done in the range 4000-400 cm⁻¹ using KBr disc. Scanning electron microscope (SEM) analysis was carried out on TiO₂-nps by KYKY (EM3200, China) electron microscope with accelerating voltage of 25kV. The morphology of TiO₂-nps was observed by Transmission electron microscope instrument (Philips, CM-200, Netherlands) with accelerating voltage of 200kV and using Field Emission Gun (FEG). The roughness of surface was obtained using angstrom AFM (SPM-AA3000, USA). The surface area measurements and pore diameter were obtained with Quantachrome Instruments (Nova 2200e, USA). The thermal stability of TiO₂-nps was performed using thermogravimetric Netzsch analyzer (TG 209 F1, Germany) in the temperature range of 45°C-659.2°C. UV-Vis spectrophotometer (UV-1800, Shimadzu, Japan) was utilized to record the spectra of prepared TiO₂-nps in range from 300 to 600 nm.

RESULTS AND DISCUSSION

Fig.1 shows the XRD pattern of TiO₂-nps. All diffraction peaks were well indexed to purely anatase phase according to standard JCPDS card No. 21-1272. No characteristic peaks were detected for rutile phase, brookite phase, or any impurities. The crystalline size and the average particle size (D) of TiO₂-nps was estimated from the width of diffraction peak at 25.4° using Debye-Scherrer equation [15]:

$$D = \frac{k\lambda}{\beta \cos \theta} \quad (1)$$

Where k is the shape factor (0.94), λ is the wavelength of X-ray irradiation (0.15040nm for CuK_α), β is full width at half maximum (FWHM), θ is the Bragg's diffraction angle at maximum peak.

The Raman spectrum (Fig. 2) of self-synthesized TiO₂ nanoparticles shows anatase bands 144, 194, 397, 517, 513, 639 cm⁻¹ without any band for rutile or brookite phase. The peak located at 639 cm⁻¹ (E_g) for Ti-O stretching mode,

the peak at 517 cm^{-1} ($A_{1g} + B_{1g}$) refer to Ti-O stretching mode, and the peak appeared at 397 cm^{-1} (E_g) assigned to the O-Ti-O bending mode [25].

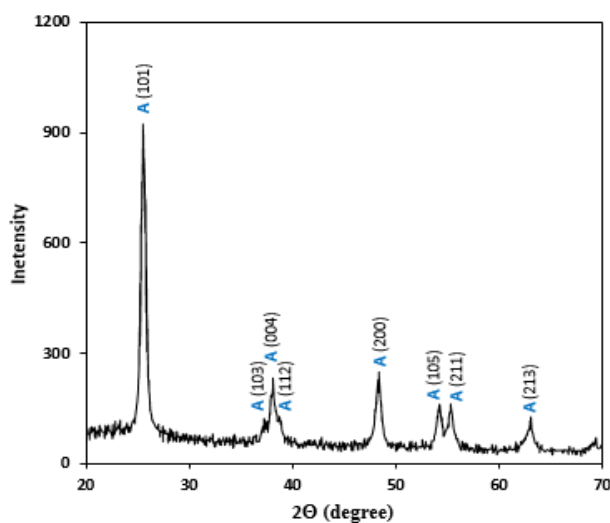


Fig. 1. X-ray diffraction (XRD) pattern of synthesized TiO_2 -nps

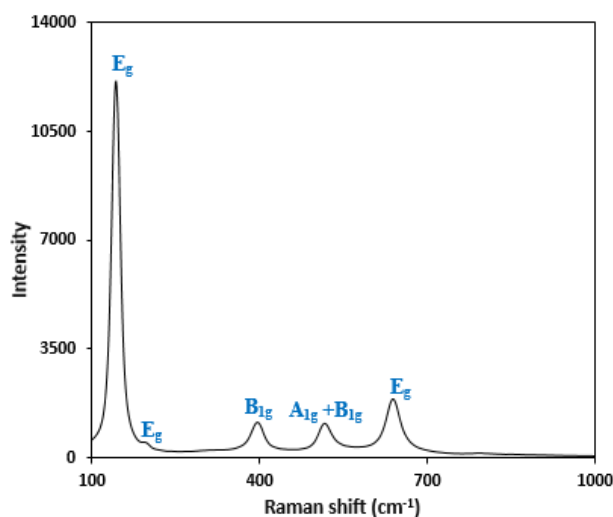


Fig. 2. Raman spectrum of anatase titania

The FTIR spectrum of TiO_2 nanoparticles was shown in Fig. 3. The broad band centered at $500\text{-}600\text{ cm}^{-1}$ is assigned to the bending vibration (Ti-O-Ti) bonds in the TiO_2 lattice. The broad band centered at $3600\text{-}3400\text{ cm}^{-1}$ assigned to the intermolecular interaction of hydroxyl group for water molecule with TiO_2 surface. The peak at 1650 cm^{-1} refer to characteristic bending vibration of -OH group [26].

The surface morphology of prepared TiO_2 -nps was characterized by SEM analysis as shown in Fig. 4. The synthesized particles have a spherical shape with good dispersion. Less agglomeration of nanoparticles was also appeared, this may be due to aggregation of primary TiO_2 particles at high calcination temperature which is necessary to accelerate the crystal growth of titanium dioxide. [27]

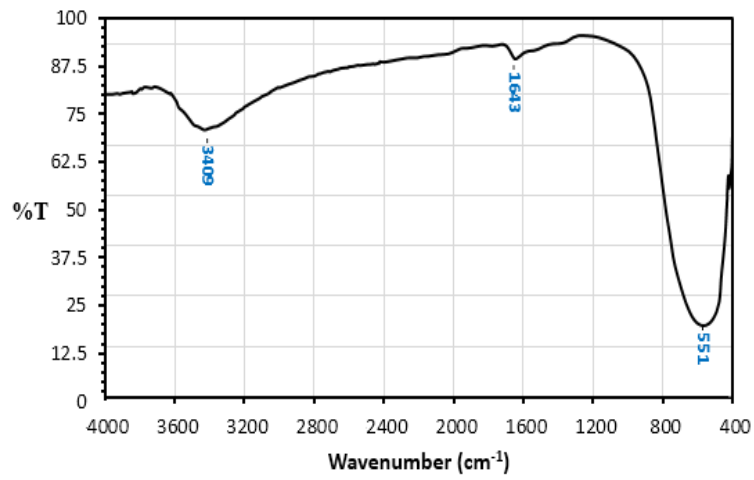


Fig.3. FTIR spectrum of TiO₂-nps

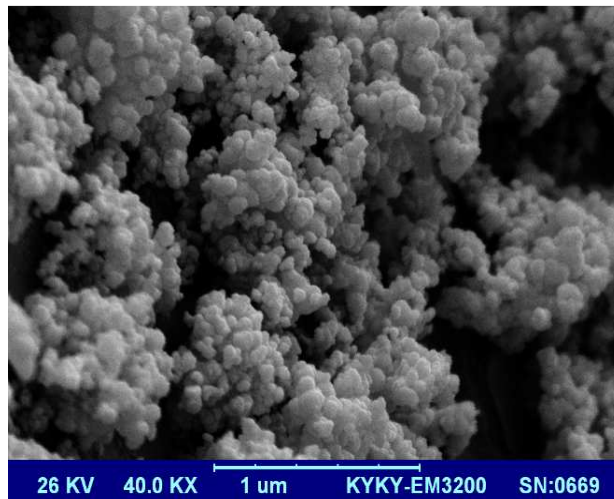


Fig. 4. SEM image of TiO₂ powder

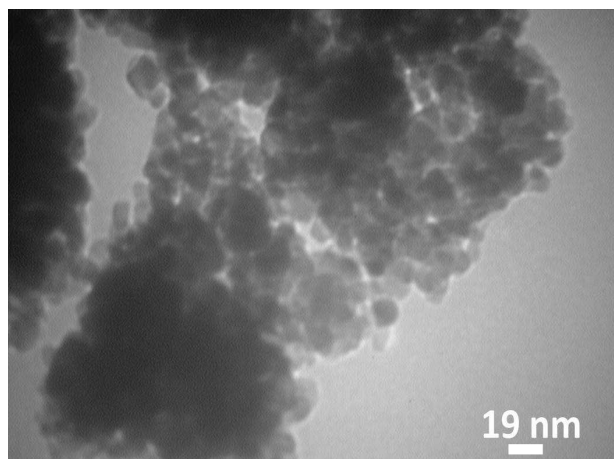


Fig. 5. TEM typical image of TiO₂-nps

The crystalline, particles size and the distribution of TiO_2 -nps was shown in TEM image (Fig. 5). TEM image shows the spherical shape with different particle size. The aggregation was shown in TEM image due to the sintering of crystals which is formed through the calcination step. The small particle size is approximately equal to 11 ± 5 nm.

The surface morphology of TiO_2 -nps was also examined by AFM. Fig.6 shows the 3D image of TiO_2 -nps using tapping mode. The AFM image shows high uniform distribution of particles with spherical shape. The statistical roughness analysis (CSPM) shows that the obtained roughness average is 0.422nm, root mean square roughness is 0.513nm, surface skewness is - 0.0806, and the surface kurtosis is equal to 2.47. The AFM results show that the surface of TiO_2 is bumpy and the valleys are more than the peaks of surface [28].

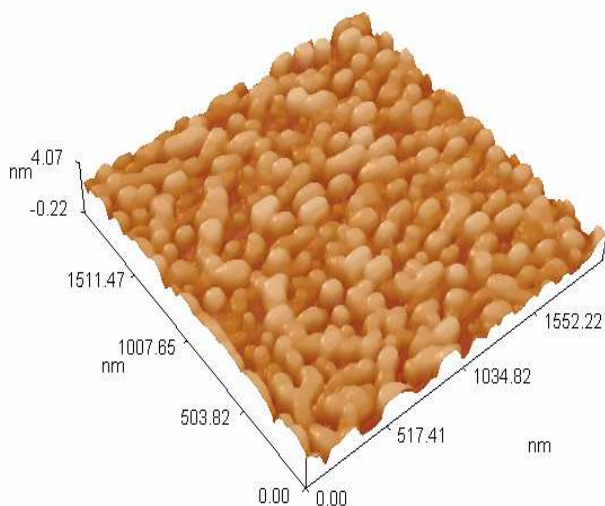


Fig. 6. AFM-3D image of TiO_2 -nps

The specific surface area of TiO_2 -nps that calculated from multi-point BET plot is $64.041 \text{ m}^2/\text{g}$. The adsorption/desorption isotherms of titania nanoparticles and the pore size distributions (inset) was shown in Fig.7. The isotherms show the type IV curve with a H1 hysteresis loop ($0.4 < P/P_0 < 0.95$), this mean that the surface includes a geometrical cylindrical pore with a high degree of pore size uniformity. The result indicated that surface has two different type of pores, mesopores (diameter 2-50nm) and micropores (diameter < 2) [29].

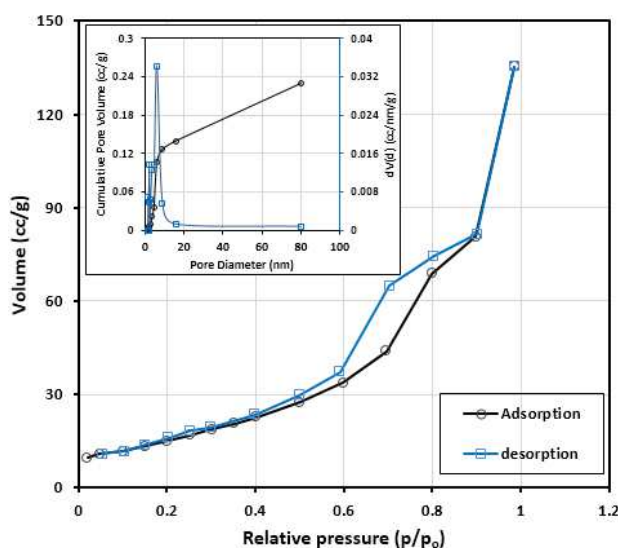


Fig. 7. The nitrogen adsorption/desorption isotherms and the pore size distribution (inset) of TiO_2 -nps

Thermal behavior of synthesized TiO₂ nanoparticles was analyzed through TGA and DTG analysis. From Fig. 8, TGA of TiO₂ was found to have a 0.00 weight loss in range 45 °C to 542 °C. This may be due to the very high thermal stability and highly purity of TiO₂ nanoparticles without any organic or water that may be attach on the surface of the sample. The significantly weight loss (0.1%) was observed at 558°C, the rate of weight loss increased after 560C° until the last degree measured 697°, the total weight loss of TiO₂ nanoparticles after completely TGA analysis was (3.44%).

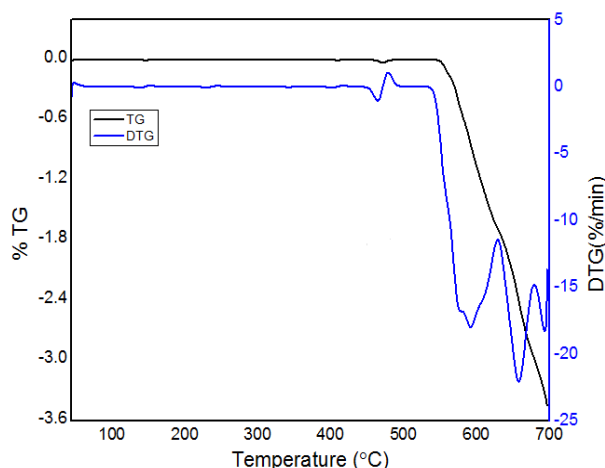


Fig. 8. TG and DTG curves of titania nanoparticles

UV-Vis absorbance spectrum of TiO₂ is shown in Fig.9. The synthesized TiO₂ shows a strong absorption in UV region. The absorbance on set value for TiO₂ was estimated by extrapolating the absorbance edge, it was found to be 388 nm. The band gab of synthesized TiO₂ can be calculated by Tauc's plot which is expressed as follows [30]:

$$(\alpha h\nu)^{1/n} = C \times (h\nu - E_g) \quad (2)$$

Where α is the absorption coefficient, h is Planck's constant, ν is frequency ($\nu = c/\lambda$, c light speed, λ is the wavelength). $n = 1/2$, and 2 for direct and indirect optical bandgab, respectively. C is proportionality constant, and E_g is bandgab. The band gab of synthesized TiO₂ nanoparticles was equal to 3.2 eV.

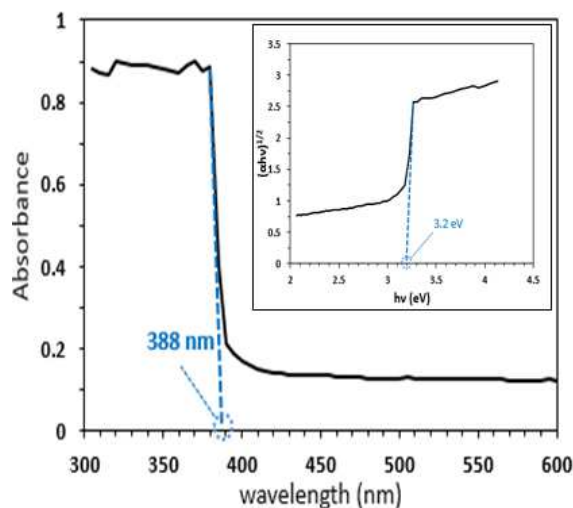


Fig. 9. UV-Vis absorbance spectrum and Tauc's plot (inset) of TiO₂ nanoparticles

CONCLUSION

A new route of sol gel method is performed for synthesis pure anatase TiO₂ nanoparticles with high quality production. The synthesis conditions was carried out using ultrasound through sol-gel technique at low temperature and acidic media. This procedure is mild, time saving, and produce pure anatase phase of TiO₂ with low particle size and less aggregation.

Acknowledgements

We sincerely express our gratitude to Professor Hassan A. Habeeb Alshamsi and university of Al-Qadisiyah, college of Science, chemistry Department for their valuable support to complete this work successfully.

REFERENCES

- [1] R.Ebrahimi,G. Tarhandeh, Rafiey, S. Narjabadi M.,H. Khani,*J. Korean Chem. Soc.*, **2012**, 56(1), 92-101.
- [2] M. A. M. L. Jesus, J. T. S. T. Neto,G.Timò,P. R. P. Paulo, M. S. Dantas, A. M. Ferreira.*Appl Adhes Sci*, **2015**, 5(3), 1-9.
- [3]Z. Zhao, G. Liu, B. Li, L. Guo, C. Fei, Y. Wang, L. Lv, X. Liu, J. Tianab, G. Cao. *J. Mater. Chem. A*, **2015**, 3, 11320-11329.
- [4]M. Pelaez, N. T. Nolan., S. C. Pillai,M. K. Seery,P. Falaras, A. G. Kontos, P. S.M. Dunlop,J.W.J. Hamilton,J.A. Byrne, K. O'Shea,M. H. Entezari;,D. D. Dionysiou. *Appl Catal B*, **2012**, 125, 331-349.
- [5],G. Cui,W. Wang,M. Ma,M. Zhang,X. Xia,F. Han,X. Shi,Y. Zhao,Y. Dong,B. Tang.*Chem. Commun.*, **2013**, 49, 6415-6417.
- [6] A.O. Ibadon, P. Fitzpatrick.*Catalysts*, **2013**, 3, 189-218.
- [7]T. Fröschl,U. Hörmann,P. Kubiak,G. Kučerová,M. Pfanzelt,C. K. Weiss,R. J. Behm,N. Hüsing,,U. Kaiser, K. Landfesterd,M. Wohlfahrt-Mehrens. *Chem. Soc. Rev.*, **2012**, 41, 5313-5360.
- [8] M.V. Dozzi, E. Selli.*Catalysts*, **2013**, 3, 455-485.
- [9] J. LIU. *Optoelectron Adv Mat*,**2011**, 5(3), 291-295.
- [10] D. A. H. Hanaor,C. C Sorrell.*J. Mater. Sci.*, **2011**, 46(4), 855-874.
- [11]A. Karami. *J Iran Chem Soc*, **2010**, 7(2), 154-160.
- [12] W. Kongsuebchart, P. Praserttham, J. Panpranot, A. Sirisuk, P. Supphasrirongjaroen, C. Satayaprasert, *J. Cryst. Growth.*, **2006**, 297(1), 234-238.
- [13] M.N. An'amt, N.M. Huang, S. Radiman,H.N. Lim, M.R. Muhamad. *Sains Malays*, **2014**, 43(1), 137-144.
- [14]H. Arami,M. Mazloumi,R. Khalifehzadeh,S.K. Sadrmezhaad. *Mater Lett*,**2007**, 61, 4559-4561.
- [15] Y. Tao, Z.N. Han, Z.L. Cheng; Q.S. Liu, F.X. Wei, K.E. Ting,X.J. Yin. *J. Chem. Eng. Mater. Sci.*, **2015**, 3, 29-36.
- [16] K. Thangavelu, R. Annamalai,D. Arulnandhi. *IJREAT*,**2008**, 3, 636-639.
- [17] H. Qu, S. Bhattacharyya, P. Ducheyne. Sol-Gel Processed Oxide Controlled Release Materials, In *Comprehensive Biomaterials*, Elsevier, Oxford, **2011**, 475-495.
- [18] V.Uche. *Adv. appl. sci. res.*, **2013**, 4(1), 506-510.
- [19] E.L.S.da Rosa.*BMC Biophysics*, **2013**, 6(11), 1-11.
- [20] J. H Bang, K. S. Suslick. *Adv. Mater.*, **2010**, 22, 1039-1059.
- [21] J. C. Yu, J. Yu, W. Hoa, L. Zhang. *Chem. Commun.*, **2001**, 1942-1943.
- [22]J. Li, T.Momono. *Mater Sci Tech*, **2005**, 21(01), 47-52.
- [23] A.B. H Yoruç, Y. Ipek. *Acta. Phys. Pol. A*, **2012**, 121(1), 230-232.
- [24] K. Zhu,M. Zhang, Q. Chen;Z. Yin.*Phys. Lett.*, **2005**, 340, 220-227.
- [25] F. Li, Y. Gu.*Mater Sci Semicond Process*, **2012**, 15, 11-14.
- [26] V.Vetrivel, K. Rajendran, V. Kalaiselvi.*Int J ChemTech Res.*, **2015**, 7(3), 1090-1097.
- [27]Y.F. Chen,C.Y. Lee,M.Y. Yeng,H.T. Chiu. *J. Cryst. Growth*, **2003**, 247, 363-370.
- [28]N. Tayebi, A. P. Andreas. *Tribol Int*, **2004**, 37, 491-505.
- [29] S.M. Zanetti, K.O. Rocha, J.A.J. Rodrigues, E. Longo.*Sens Actuators B Chem*, **2014**, 190, 40-47.
- [30]C. Kim,H. Jeong. *Bull. Korean Chem. Soc.*, **2007**, 28(12), 2333-2337.